



The 72-h WEBT microvariability observation of blazar S5 0716+714 in 2009

Bhatta et al.(2013)

Reporter: Xin Chang (常鑫)

email: cx@mail.ynu.edu.cn

Yunnan University

SWIFAR

2024-03-19

Introduction

1. The international Whole Earth Blazar **Telescope (WEBT)** consortium carried out three days of intensive micro-variability observations of S5 0716+714 from February 23 to 26, 2009.
2. Thirty-six observatories in sixteen countries participated in this continuous monitoring program and twenty of them submitted data for compilation into a continuous light curve.
3. The light curve was analyzed using several techniques including Fourier transform, Wavelet and noise analysis techniques.
4. They obtained an excellent fit to the 72-hour light curve with the synchrotron pulse model.

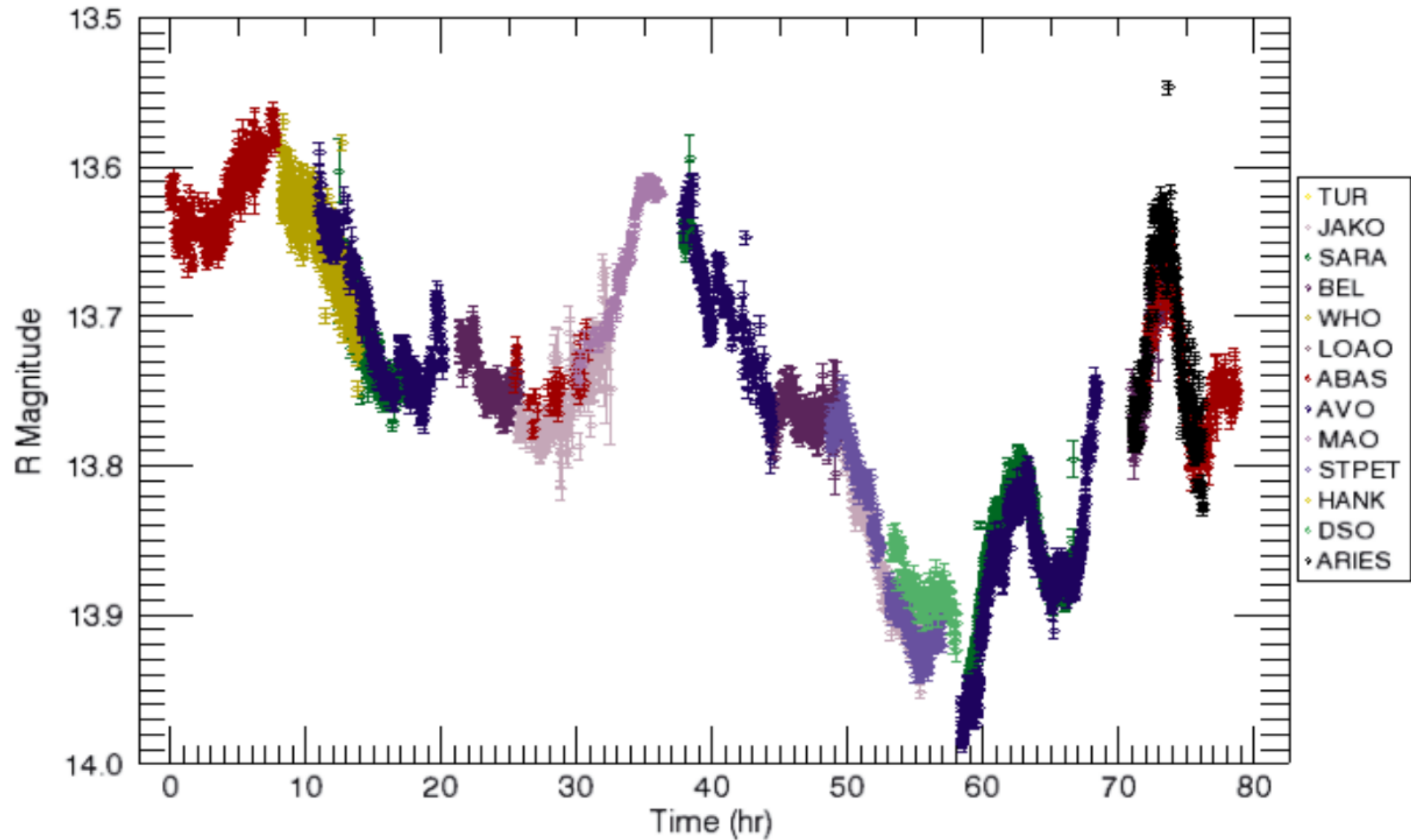
Observation

Observatories contributing observations to the WEBT campaign.

| Zone | Code | Country | Observatory | Longitude | Telescope | Filters |
|------|-------|--------------|--------------------------|-----------|-------------|-------------|
| 1 | AAS | Spain | Agrupacion Obs. | 0.73 | 0.5 m | <i>R</i> |
| 1 | AVO | Italy | Aosta Valley Obs. | 7.36 | 0.81-m | <i>RI</i> |
| 1 | MAO | Germany | Michael Adrian Obs. | 8.41 | 1.2-m | <i>BVRI</i> |
| 2 | AAO | Italy | Armenzano Obs. | 12.69 | 36-cm | <i>R</i> |
| 3 | TUR | Finland | Tuorla Observatory | 22.17 | 35-cm, 1-m | <i>R</i> |
| 3 | BEL | Bulgaria | Belogradchik | 22.60 | 60-cm | <i>BVRI</i> |
| 3 | HANK | Finland | Hankasalmi | 26.50 | 40-cm (RC) | <i>BVRI</i> |
| 3 | STPET | Russia | St. Petersburg | 29.82 | 40-cm | <i>R</i> |
| 3 | JAKO | Finland | Jakokoski Obs. | 30.00 | 20-inch | <i>I R</i> |
| 4 | CRIM | Crimea | Crimean AP Obs. | 30.20 | 2.6, 1.25 m | <i>R</i> |
| 5 | ABAS | Georgia, FSU | Abastumani Obs. | 42.80 | 0.7-m | <i>R</i> |
| 6 | ARIES | India | ARIES | 71.68 | 1.04 m | <i>R</i> |
| 7 | BAO | China | BAO China, Xinglong | 114.00 | 1.0-m | <i>R</i> |
| 7 | WHO | China | Weihai China | 122.00 | 1-m | <i>BVRI</i> |
| 8 | LOAO | USA | Mt. Lemmon | 249.00 | 1.0-m | <i>R</i> |
| 11 | MDM | USA | MDM Kitt Peak | 249.00 | MDM 1.3 m | <i>R</i> |
| 11 | SARA | USA | SARA/Kitt Peak | 249.00 | 1.-m | <i>R</i> |
| 12 | BUO | USA | Butler | 273.55 | 0.96-m | <i>R</i> |
| 12 | DSO | USA | Dark Sky, North Carolina | 278.58 | 24-inch | <i>R</i> |
| 13 | BLK | Ireland | Cork | 352.00 | 40-cm | <i>RGB</i> |

1. This table lists 16 countries with different observing codes, observatory name, telescope longitude, telescope size and filters.
2. The code is the key to the observatories responsible for each data segment on the plot.

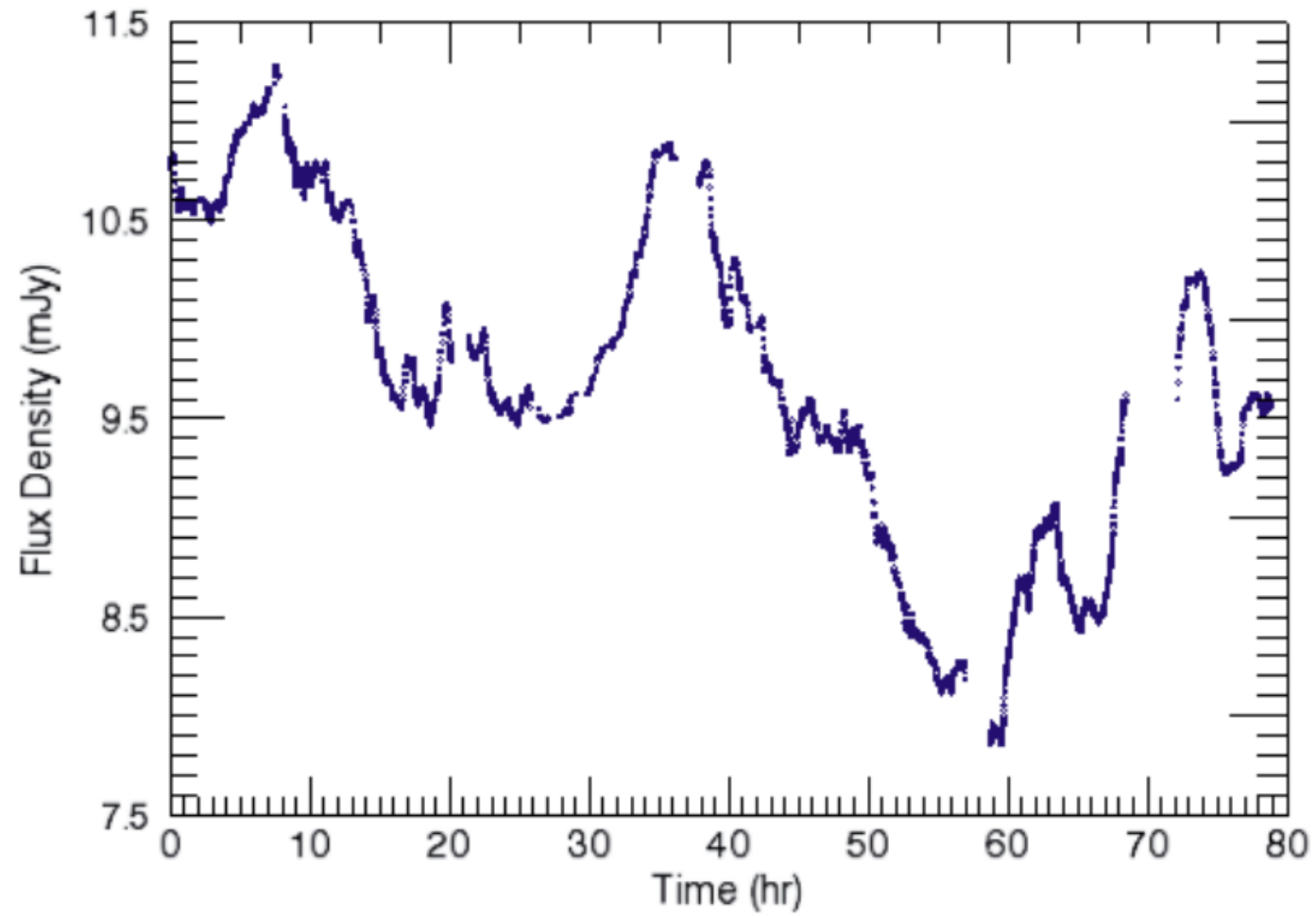
Observation



Observation

1. Figure 1 shows the raw observations plotted together.
2. The observations covered the time period from February 23 to 26 in 2009.
3. They made minor zero-point adjustments to obtain a consistent continuous light curve.
4. Exposure times for individual images ranged from 30 s to 120 s depending on the observatory and telescope.

Observation



Observation

- Figure 2 shows the complete flux curve.
- **The magnitudes were converted to flux using standard flux conversions for the R filter** as given by Johnson (1966) using a redshift of 0.30 and Galactic absorption of 0.031 mag.
- The total length of the light curve was 78.88 h. They analyzed individual segments of the flux curve to determine the maximum climb and decline rates.

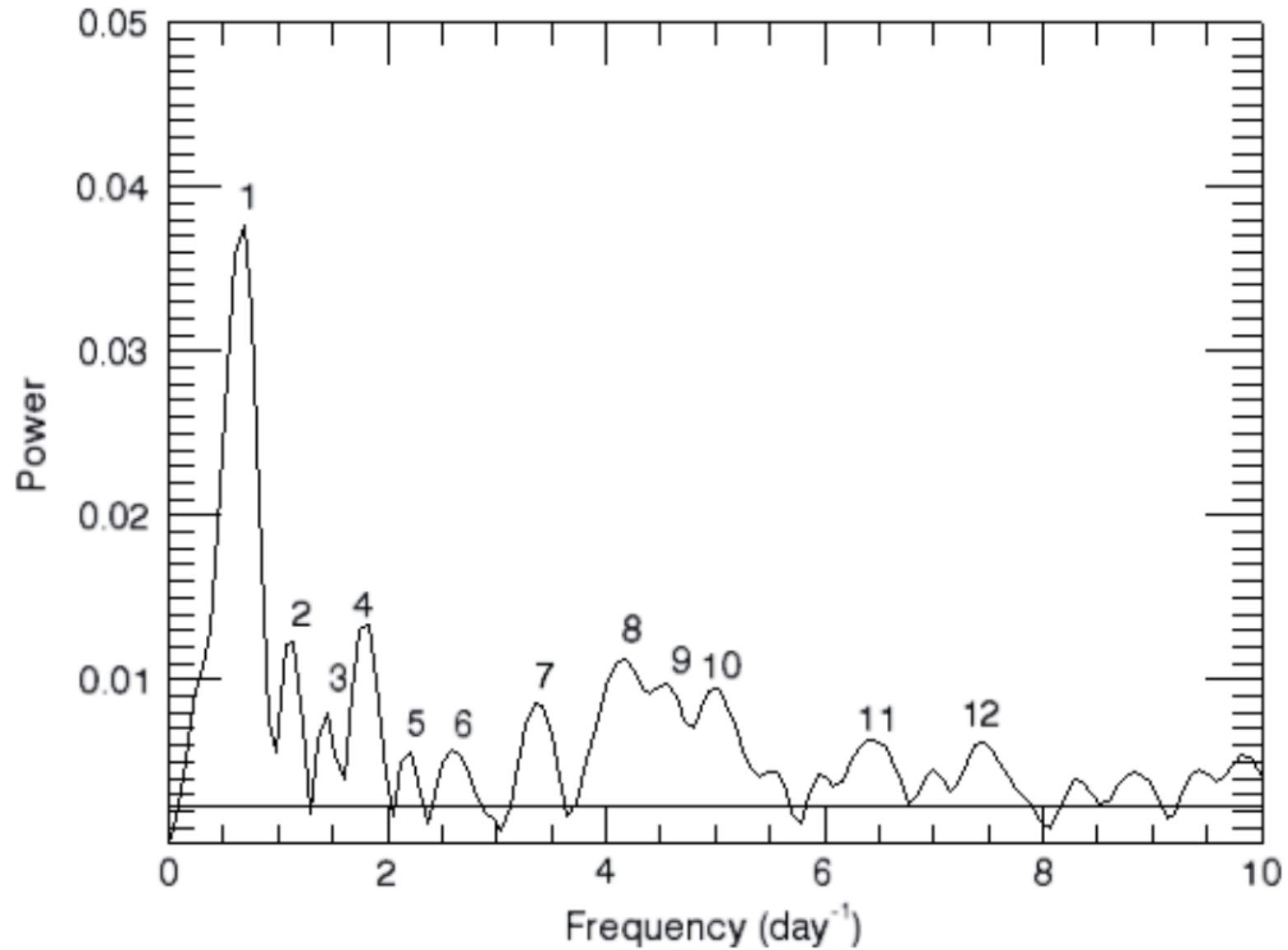
Observation

| Seg | Times (h) | Slope (mag/h) | r^2 | Npts | Prob. | Rise/Decline |
|-----|--------------|------------------|-------|------|--------------------|--------------|
| 1 | 3.38–7.01 | 0.019 | 0.918 | 123 | 5×10^{-7} | Rise |
| 2 | 13.03–16.54 | 0.027 | 0.946 | 155 | 5×10^{-7} | Decline |
| 3 | 18.69–19.84 | 0.064 | 0.967 | 40 | 1×10^{-6} | Rise |
| 4 | 29.91–35.76 | 0.029 | 0.968 | 120 | 1×10^{-6} | Rise |
| 5 | 38.39–39.91 | 0.050 | 0.945 | 77 | 5×10^{-7} | Decline |
| 6 | 49.70–55.30 | 0.022 | 0.956 | 177 | 5×10^{-7} | Decline |
| 7 | 58.52–63.10 | 0.037 | 0.878 | 244 | 5×10^{-7} | Rise |
| 8 | 63.48–65.20 | 0.033 | 0.904 | 115 | 5×10^{-7} | Decline |
| 9 | 66.74–68.46 | 0.089 | 0.977 | 99 | 5×10^{-7} | Rise |
| 10 | 72.14–73.60 | 0.035 | 0.739 | 29 | 1×10^{-6} | Rise |
| 11 | 74.07–75.63 | 0.076 | 0.977 | 43 | 1×10^{-6} | Decline |
| 12 | 75.66–78.17 | 0.026 | 0.873 | 73 | 5×10^{-7} | Rise |

Observation

- Table 2 lists the slopes and correlation coefficients for each climb and decline segments.
- Col. 2: the start and finish time of the segment in hours
- Col. 3: the slope
- Col. 4: the correlation coefficient for each fit
- Col. 5: the number of points.
- Col. 6: the probability of correlation coefficient.
- column 7 denotes whether the slope is a rise or a decline.
- **The results show that** the average decline rate was 0.042 mag/h (standard deviation of 0.022) while the average rise rate was 0.043 with a standard deviation of 0.028. Thus over all, **the rise and decline rates are similar in this segment of light curve.**
- Although the rates are different, the fact that the slopes for the rise and decline are the same agree with the results found by Villata et al. (2000) and Montagni et al. (2006).

Time series analysis



Time series analysis

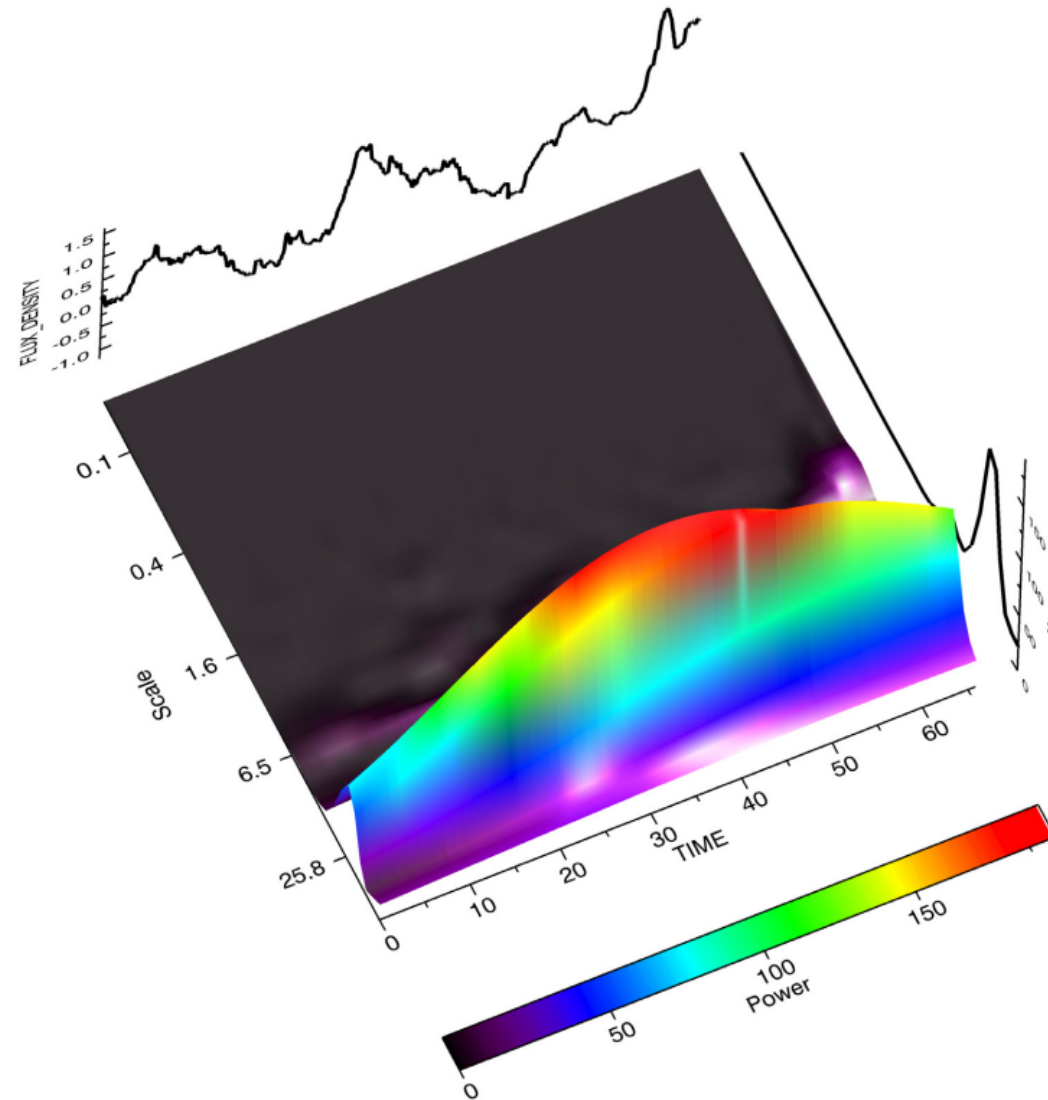
| Number | Frequency (/day) | Power | Timescale in obs. frame (h) | Timescale in rest frame (h) |
|--------|---------------------|--------|--------------------------------|--------------------------------|
| 1 | 0.60 | 0.0382 | 40.00 | 656.00 |
| 2 | 1.14 | 0.0122 | 21.05 | 345.22 |
| 3 | 1.41 | 0.0083 | 17.02 | 279.13 |
| 4 | 1.82 | 0.0126 | 13.19 | 216.32 |
| 5 | 2.25 | 0.0052 | 10.67 | 174.99 |
| 6 | 2.60 | 0.0054 | 9.23 | 151.37 |
| 7 | 3.40 | 0.0081 | 7.06 | 115.78 |
| 8 | 4.20 | 0.0121 | 5.71 | 93.64 |
| 9 | 4.54 | 0.0092 | 5.29 | 86.76 |
| 10 | 5.00 | 0.0091 | 4.80 | 78.72 |
| 11 | 6.50 | 0.0063 | 3.69 | 60.52 |
| 12 | 7.50 | 0.0062 | 3.20 | 52.48 |

Time series analysis

- **Fourier transform analysis**
- **They performed Fourier transform analysis on the entire light curve** by using a discrete Fourier transform (DFT) algorithm (Deeming 1975).
- The results of this analysis are shown in Fig. 3 and Table 3.
- **From the results we can see 12 peaks exceeding the horizontal line across the bottom which indicates the peaks exceeding the average power of 100 light curves.**
- Column 4 indicates the time scales of these twelve peaks.
- Column 5 indicates the corresponding time-scales in the rest frame calculated using:

$$\Delta t_{\text{rest}} = \frac{D}{1+z} \Delta t_{\text{obs}} \quad \longleftarrow \quad D = 1/\Gamma (1 - \beta \cos \theta)$$

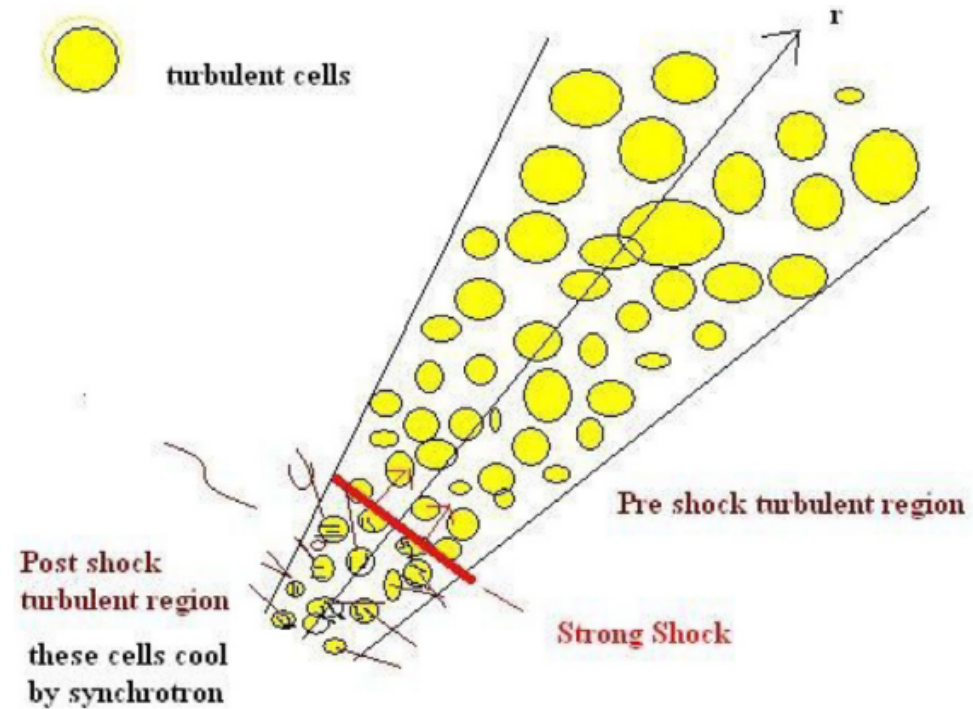
Time series analysis



Time series analysis

- Figure 4 shows the result of wavelet transform analysis (Torrence & Compo 1998).
- From this figure we can see the peak is clearly only significant in the center of the data, fitting extremely poorly at the start or end of the light curve.
- **They did not find the periods** at approximately 25 and 73 min in this flux curve seen previously by Gupta et al. (2009). **Thus they could not confirm any of the previously detected periods seen in the S5 0716+714.**
- So, they propose a new model for the interpretation of microvariability.

Modeling the microvariations



Shock acceleration of electrons and amplification of magnetic fields parallel to the shock front in turbulent cells.

Yields synchrotron cooling in post-shock region from shocked cells.

Modeling the microvariations

- They investigate a model that:

plasma blobs can be generated by magnetic reconnection in the jet. When shocks in the jet interact with plasma blobs, they induce changes in density and temperature, resulting in radiation emission.

The rapid particle acceleration and subsequent cooling by synchrotron emission produces a pulse in the flux curve.

Modeling the microvariations

- The particle distribution function of this model given by Ball & Kirk (1992).

$$\frac{\partial N}{\partial t} + \frac{\partial}{\partial \gamma} \left[\left(\frac{\gamma}{t_{\text{acc}}} - \beta_s \gamma^2 \right) N \right] + \frac{N}{t_{\text{esc}}} = Q \delta(\gamma - \gamma_0)$$

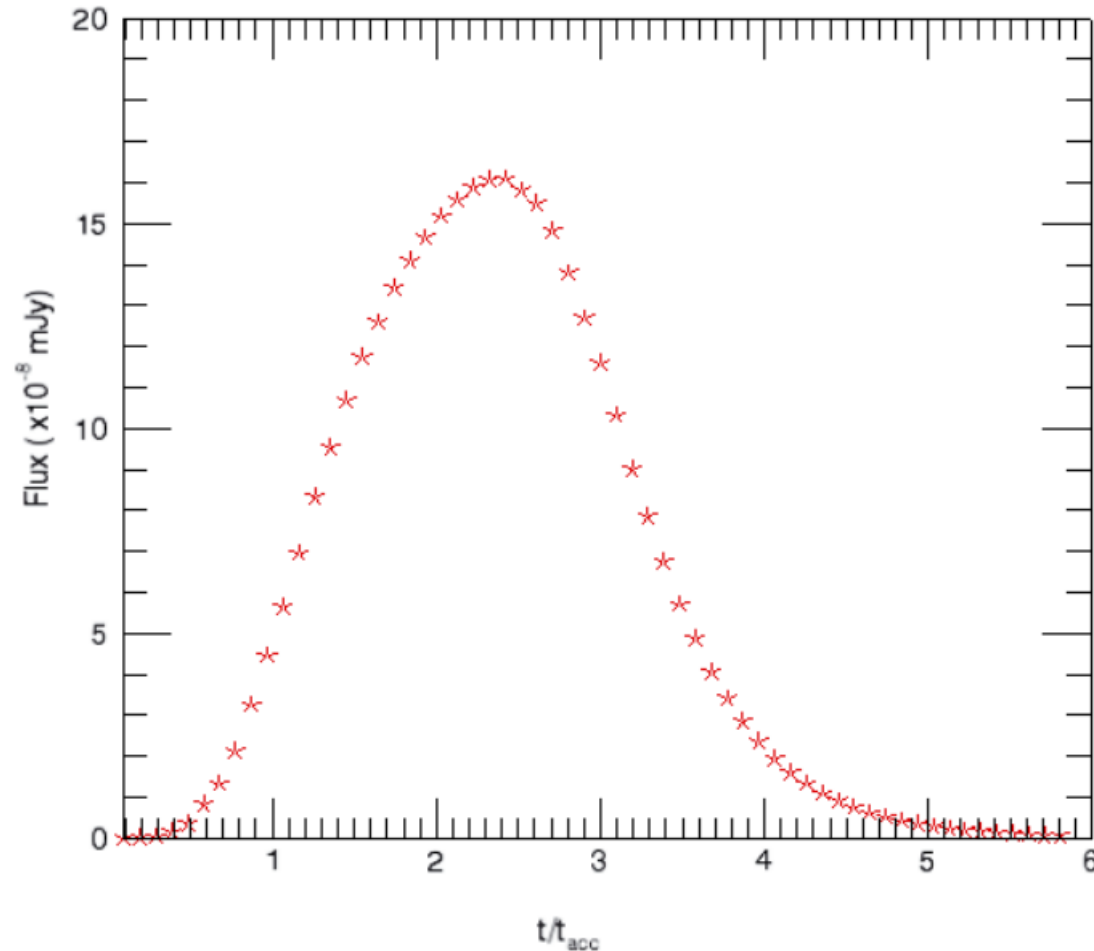
with

$$\beta_s = \frac{4}{3} \frac{\sigma_T}{m_e c} \left(\frac{B^2}{2\mu_0} \right)$$

- KRM (Kirk et al. 1998) calculated the particle acceleration in the shock front for various magnetic field orientations and particle densities assuming a plane shock encounters a cylindrical density enhancement.
- **In this model, the ratio of the acceleration time t_{acc} and escape time t_{esc} , in addition to constraints on the cooling length L control the pulse shape.**
- **The amplitude is given by the parameter Q and is related to the magnetic field strength B and orientation θ in addition to the enhanced electron density.**

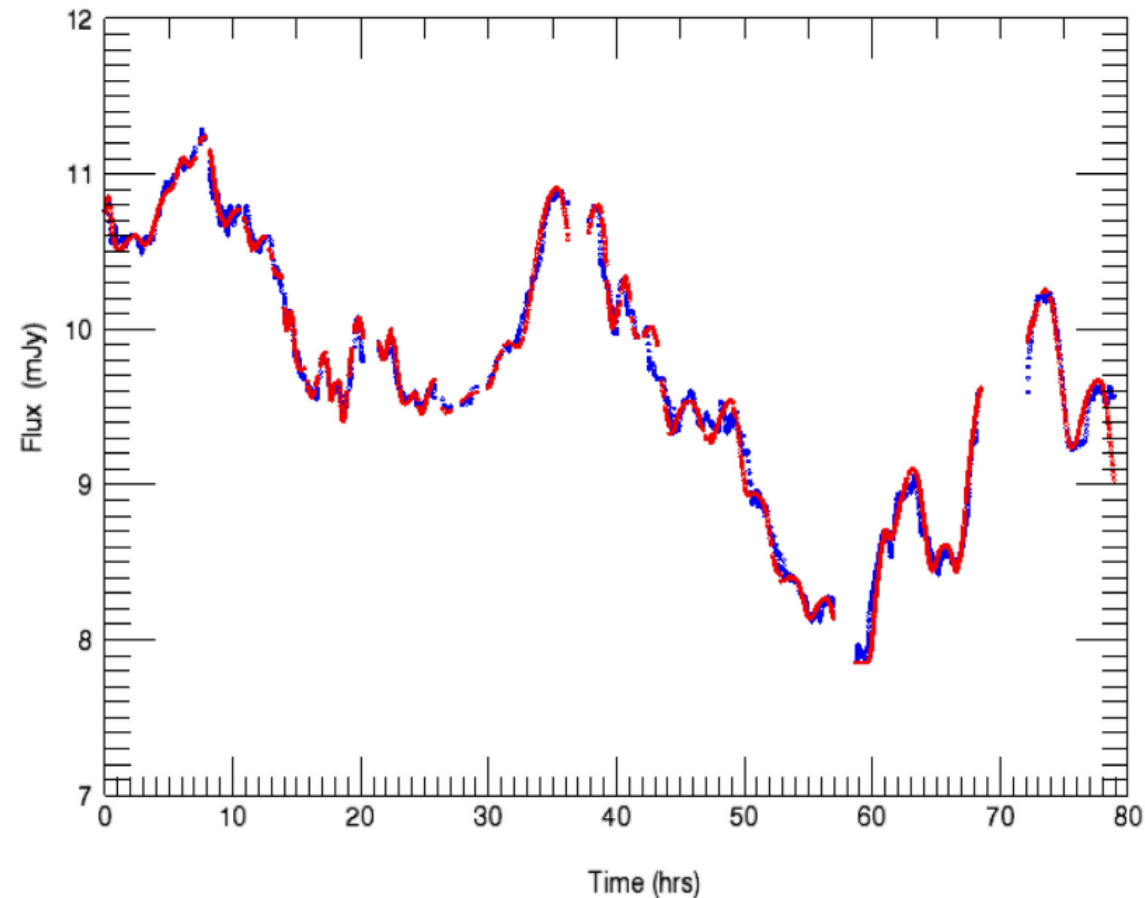
Modeling the microvariations

- After a number of test solutions, they determined that for $t_{acc}/t_{esc} = 0.5$ they get **symmetric** pulse shapes similar to what they see in the microvariability curves. The pulse shape is shown in Fig. 8. They used this as the standard pulse shape for all subsequent fits.



Modeling the microvariations

- They fit thirty-five pulses to the microvariability curve by varying the width and amplitude of the standard pulse. This Figure shows the light curve fitted with the convolved pulses. The blue points are the smoothed data and the red points are the model. The fit correlation coefficient is 0.98. Since turbulence is a stochastic process, each microvariability curve is a realization of that stochastic process.



Modeling the microvariations

| Pulse | Center (h) | Amp (mJy) | τ_{flare} (h) | N $\times 10^{-5}(\text{s}^{-1} \text{m}^{-3})$ | S_{cell} AU | Index |
|-------|---------------|--------------|------------------------------|--|-------------------------|-------|
| 1 | 0.15 | 0.57 | 1.11 | 4.94 | 13.18 | 4 |
| 2 | 2.10 | 2.74 | 9.74 | 23.56 | 115.35 | 34 |
| 3 | 5.70 | 1.27 | 3.34 | 10.94 | 39.54 | 23 |
| 4 | 7.80 | 1.47 | 3.75 | 12.66 | 44.49 | 30 |
| 5 | 8.45 | 1.24 | 2.78 | 10.69 | 32.95 | 18 |
| 6 | 10.80 | 0.14 | 3.61 | 1.25 | 42.84 | 28 |
| 7 | 10.90 | 2.39 | 2.92 | 20.56 | 34.60 | 20 |
| 8 | 13.00 | 2.34 | 2.50 | 20.13 | 29.66 | 17 |
| 9 | 14.30 | 1.29 | 1.41 | 11.12 | 16.80 | 7 |
| 10 | 14.60 | 0.19 | 0.55 | 1.68 | 6.59 | 1 |
| 11 | 15.50 | 1.69 | 1.67 | 14.55 | 19.77 | 9 |
| 12 | 17.20 | 1.94 | 2.19 | 16.69 | 26.03 | 15 |
| 13 | 18.20 | 0.72 | 0.78 | 6.22 | 9.22 | 2 |
| 14 | 19.75 | 2.04 | 2.45 | 17.55 | 29.00 | 16 |
| 15 | 21.30 | 0.57 | 0.78 | 4.94 | 9.22 | 3 |

Modeling the microvariations

- The resulting parameters for the pulses used in modeling the light curve are listed in Table 4.
 - Column1 is the shot number in time order,
 - Column2 is the center time of the pulse.
 - Column3 and 4 is the amplitude and width of each of pulse
 - Column5 is the electron density enhancement
 - Column 6 is the size for the cell
-
- **The center time is related to the relative location of the cell along the jet.**
 - **There is a large range of length/time scales for the turbulent vortices. The smallest vortex timescale is normally associated with the Kolmogorov scale** (where most of the dissipation takes place in non-relativistic plasma) **and the largest length scales are associated with either the size of the plasma jet or the correlation length within the plasma.**

Thanks!